Michigan Math. J. 63 (2014), 635–667

Branched Spherical CR Structures on the Complement of the Figure-Eight Knot

Elisha Falbel & Jieyan Wang

Abstract. We obtain a branched spherical CR structure on the complement of the figure-eight knot whose holonomy representation was given in [4]. There are essentially two boundary unipotent representations from the complement of the figure-eight knot into $\mathbf{PU}(2,1)$, which we call ρ_1 and ρ_2. We make explicit some fundamental differences between these two representations. For instance, seeing the figure-eight knot complement as a surface bundle over the circle, the behavior of the fundamental group of the fiber under the representation is a key difference between ρ_1 and ρ_2.

1. Introduction

The three-dimensional sphere contained in $\mathbb{C}^2$ inherits a Cauchy–Riemann structure as the boundary of the complex two-ball. Three-dimensional manifolds locally modeled on the sphere then are called spherical CR manifolds and have been studied since Cartan [2]. Spherical CR structures appear naturally as quotients of an open subset of the three-dimensional sphere by a subgroup of the CR automorphism group (denoted $\mathbf{PU}(2,1)$) (see [8; 7] and [12] for a recent introduction).

The irreducible representations of the fundamental group of the complement of the figure-eight knot into $\mathbf{PU}(2,1)$ with unipotent boundary holonomy were obtained in [4]. To obtain such representations, the existence of a developing map obtained from the 0-skeleton of an ideal triangulation is imposed. Solution of a system of algebraic equations gives rise to a set of representations of $\Gamma = \pi_1(M)$, the fundamental group of the complement of the figure-eight knot with parabolic peripheral group.

Up to precomposition with automorphisms of Γ, there exist two irreducible representations into $\mathbf{PU}(2,1)$ with unipotent boundary holonomy (see [3]). Following [4], we call them ρ_1 and ρ_2. In [4], we showed that ρ_1 could be obtained from a branched spherical CR structure on the knot complement. Moreover, this representation is not the holonomy of a uniformizable structure since the limit set is the full sphere S^3.

In this paper, we analyze ρ_2 and show that it is also obtained as the holonomy of a branched structure in Theorem 12 in Section 6. The branched locus in the complement of the figure-eight knot is a segment with end points in the knot

Received November 26, 2013. Revision received March 15, 2014.
The second author was supported by CSC and NSF (No. 11071059).

(see Figure 8), and the fundamental group of the complement of the branched locus is easily seen to be the free group with two generators (see the beginning of Section 6).

The proof consists of extending the developing map obtained from the 0-skeleton to a developing map defined on simplices. A uniformizable (non-branched) spherical CR structure on the complement of the figure-eight knot was obtained in [3]. Although the uniformizable structure with unipotent boundary holonomy is unique (see [3]), it is not clear to us how to describe all branched structures. The motivation to study branched CR structures is the hope that they would be easier to associate to a manifold once a representation is given. Since we have a general method to construct representations of the fundamental group into $\mathbf{PU}(2,1)$, we would like an efficient method to obtain spherical CR structures with holonomy the given representation. Constructing branched structures might be a step in this process. Remark that a uniformizable structure in the Whitehead link complement is described in [12] and, more recently, in [10].

A drawback in the method we use is the fact that the choices made here in order to define tetrahedra are not canonical. In fact, we can hope that for other representations, more canonical choices will be enough to construct (possibly, branched) structures. Indeed, the fact that we use only two tetrahedra for the complement of the figure-eight knot imposes very tight conditions on the choice of the faces (this is not a triangulation of the complement since the simplices are not embedded). When the manifold is triangulated with more tetrahedra, it is possible that we might need to decide from only a finite number of choices (see Section 5.2 for examples of possible choices).

Another motivation for this paper is to emphasize a major difference between the two representations ρ_1 and ρ_2. Recall that the fundamental group of the figure-eight knot complement contains a surface group (a punctured torus group) as a normal subgroup corresponding to the fundamental group of the fiber of the fibration of the complement over a circle. In fact, the kernel of the first representation is contained in the surface group (and is not finitely generated), but the kernel of the second one is not. This, in turn, implies that the image of the surface group has infinite index in the image of ρ_1 but has finite index in the image of ρ_2. Both images of the representations are contained in arithmetic lattices as infinite index subgroups. It turns out that the limit set of the image of ρ_1 is the full S^3, but the image of ρ_2 has a proper limit set (see [3]). These properties are given in Sections 4.1 and 4.2. They might be general properties of representations of 3-manifold groups into $\mathbf{PU}(2,1)$.

2. Complex Hyperbolic Space and Its Boundary

In this section, we introduce some basic material on complex hyperbolic geometry. We refer to Goldman's book [7] for details.

2.1. Complex Hyperbolic Space and Its Isometry Group

Let $\mathbb{C}^{2,1}$ be the three-dimensional complex vector space equipped with the Hermitian form

$$\langle Z, W\rangle = Z_1\overline{W}_3 + Z_2\overline{W}_2 + Z_3\overline{W}_1.$$

We have three subspaces:

$$V_+ = \{Z \in \mathbb{C}^{2,1} : \ \langle Z, Z\rangle > 0\},$$
$$V_0 = \{Z \in \mathbb{C}^{2,1} - \{0\} : \ \langle Z, Z\rangle = 0\},$$
$$V_- = \{Z \in \mathbb{C}^{2,1} : \ \langle Z, Z\rangle < 0\}.$$

Let $P : \mathbb{C}^{2,1} - \{0\} \to \mathbb{C}P^2$ be the canonical projection onto complex projective space. Then the complex hyperbolic 2-space is defined as $\mathbf{H}^2_{\mathbb{C}} = P(V_-)$, which is biholomorphic to the unit ball in $\mathbb{C}^2$ equipped with the Bergman metric of constant negative holomorphic sectional curvature equal to -1. The boundary of complex hyperbolic space is defined as $\partial\mathbf{H}^2_{\mathbb{C}} = P(V_0)$, and it is diffeomorphic to a sphere. Indeed, using the equivalent Hermitian form

$$\langle Z, W\rangle_1 = Z_1\overline{W}_1 + Z_2\overline{W}_2 - Z_3\overline{W}_3,$$

we obtain the *ball model* of the complex hyperbolic space: We can write $P(V_-)$ in a chart with coordinates $z_1 = Z_1/Z_3$, $z_2 = Z_2/Z_3$ as

$$\{(z_1, z_2) \mid |z_1|^2 + |z_2|^2 < 1\},$$

and then its boundary is identified to the sphere

$$S^3 = \{(z_1, z_2) \mid |z_1|^2 + |z_2|^2 = 1\}.$$

Let $\mathbf{U}(2, 1)$ be the linear matrix group preserving the Hermitian form $\langle\cdot, \cdot\rangle$. The holomorphic isometry group $\mathbf{PU}(2, 1)$ of $\mathbf{H}^2_{\mathbb{C}}$ is the projectivized unitary group $\mathbf{U}(2, 1)$. The isometry group of $\mathbf{H}^2_{\mathbb{C}}$ is

$$\widehat{\mathbf{PU}(2, 1)} = \langle \mathbf{PU}(2, 1), Z \mapsto \overline{Z}\rangle,$$

where $Z \mapsto \overline{Z}$ is the complex conjugation.

The elements of $\mathbf{PU}(2, 1)$ can be classified into three classes. An element $g \in \mathbf{PU}(2, 1)$ is called loxodromic if g fixes exactly two points in $\partial\mathbf{H}^2$; g is called parabolic if it fixes exactly one point in $\partial\mathbf{H}^2$; otherwise, g is called elliptic.

2.2. Lattices

Let $\mathcal{O}_d$ be the ring of integers in the imaginary quadratic number field $\mathbb{Q}(i\sqrt{d})$ where d is a positive square-free integer. If $d \equiv 1, 2 \pmod 4$, then $\mathcal{O}_d = \mathbb{Z}[i\sqrt{d}]$, and if $d \equiv 3 \pmod 4$, then $\mathcal{O}_d = \mathbb{Z}[\frac{1+i\sqrt{d}}{2}]$. The subgroup of $\mathbf{PU}(2, 1)$, which is obtained by projectivization of the group that, up to scalars, is in $\mathbf{U}(2, 1)$ defined by matrices with entries in $\mathcal{O}_d$, is called the *Picard modular group* for $\mathcal{O}_d$ and is denoted $\mathbf{PU}(2, 1; \mathcal{O}_d)$. They are arithmetic lattices first considered by Picard.

2.3. Heisenberg Group and $\mathbb{C}$-Circles

The Heisenberg group $\mathfrak{N}$ is defined as the set $\mathbb{C} \times \mathbb{R}$ with group law

$$(z, t) \cdot (z', t') = (z + z', t + t' + 2\,\mathrm{Im}(z\overline{z}')).$$

The boundary of the complex hyperbolic space $\partial\mathbf{H}^2_{\mathbb{C}}$ can be identified with the one-point compactification $\overline{\mathfrak{N}}$ of $\mathfrak{N}$. Indeed, $\mathbf{PU}(2, 1)$ acts on the boundary with an isotropy group at a point that contains the Heisenberg group $\mathfrak{N}$ acting simply transitively on the complement of that point.

A point $p = (z, t) \in \mathfrak{N}$ and the point at infinity are lifted to the following points in $\mathbb{C}^{2,1}$:

$$\hat{p} = \begin{bmatrix} (-|z|^2 + it)/2 \\ z \\ 1 \end{bmatrix} \quad \text{and} \quad \hat{\infty} = \begin{bmatrix} 1 \\ 0 \\ 0 \end{bmatrix}.$$

There are two kinds of totally geodesic submanifolds of real dimension 2 in $\mathbf{H}^2_{\mathbb{C}}$, complex geodesics and totally real totally geodesic planes. Their boundaries in $\partial\mathbf{H}^2_{\mathbb{C}}$ are called $\mathbb{C}$-circles and $\mathbb{R}$-circles. Complex geodesics can be parameterized by their polar vectors, that is, points in $P(\mathbb{C}^{2,1})$ that are projections of vectors orthogonal to the lifted complex geodesic.

The Heisenberg group will be called *the Heisenberg model* when identified to the boundary of complex hyperbolic space with one point deleted.

PROPOSITION 2.1. *In the Heisenberg model, $\mathbb{C}$-circles are either vertical lines or ellipses whose projections on the z-plane are circles.*

For a given pair of distinct points in $\partial\mathbf{H}^2_{\mathbb{C}}$, there is a unique $\mathbb{C}$-circle passing through them. Finite $\mathbb{C}$-circles are determined by a center and a radius. For example, the finite $\mathbb{C}$-circle with center (z_0, t_0) and radius $R > 0$ has a polar vector

$$\begin{bmatrix} (R^2 - |z_0|^2 + it_0)/2 \\ z_0 \\ 1 \end{bmatrix},$$

and in it any point (z, t) satisfies the equations

$$\begin{cases} |z - z_0| = R, \\ t = t_0 + 2\,\mathrm{Im}(\overline{z}z_0). \end{cases}$$

2.4. CR Structures

CR structures appear naturally as the boundaries of complex manifolds or as real submanifolds of complex manifolds. The local geometry of these structures was studied by Cartan [2], who defined, in dimension three, a curvature analogous to curvatures of a Riemannian structure. When that curvature is zero, Cartan called them spherical CR structures and developed their basic properties. A much later study by Burns and Shnider [1] contains the modern setting for these structures (based on the notion of (G, X)-structures, which we will refer to as *geometric*

structures). In fact, as it was already clear to Cartan, being of zero curvature is equivalent to the following definition.

DEFINITION 2.1. A spherical CR-structure on a 3-manifold is a geometric structure modeled on the homogeneous space S^3 with the above $\mathbf{PU}(2,1)$ action (i.e., a $(\mathbf{PU}(2,1), S^3)$-structure).

Here S^3 is seen as the boundary of complex hyperbolic space in the ball model (see Section 2).

An important feature of the model manifold is the fact that it has a contact distribution given by $TS^3 \cap JTS^3$ where $J : \mathbb{C}^2 \to \mathbb{C}^2$ is the complex structure in $\mathbb{C}^2$ given by multiplication by i. This contact structure induces a contact structure on a manifold with a CR-structure. Although we are not going to make use of this observation in this paper, it is interesting to note that $\mathbb{C}$-circles are transverse to the contact distribution whereas $\mathbb{R}$-circles are tangent to it.

DEFINITION 2.2. We say a spherical CR-structure on a 3-manifold is uniformizable if it is equivalent to a quotient of the domain of discontinuity in S^3 of a discrete subgroup of $\mathbf{PU}(2,1)$.

We recall that the domain of discontinuity is the maximal open set where the action of the group is properly discontinuous. Here, equivalence between CR structures is defined as in general (G, X)-structures. Namely, we say that two CR structures are equivalent if there exists a diffeomorphism between them such that composition with charts in the target gives charts in the source that are compatible with the original structure in the source. Observe that taking the complex conjugate of local charts of a CR structure (maps of open sets into S^3) gives another CR structure that might not be equivalent to the original one but give equivalent $(\widehat{\mathbf{PU}(2,1)}, S^3)$-structures.

A CR structure, in particular, has an orientation that is compatible with the orientation induced by its contact structure. Observe that even $\widehat{\mathbf{PU}(2,1)}$ preserves orientation, so a $(\widehat{\mathbf{PU}(2,1)}, S^3)$-structure is also oriented. Both orientations of S^3 are obtained via equivalent CR structures because there exists an orientation-reversing diffeomorphism of S^3. More generally, CR structures on manifolds that have orientation-reversing maps will have equivalent CR structures inducing both orientations. In particular, the fact that the figure-eight knot is amphicheiral means precisely that there exists an orientation-reversing diffeomorphism of S^3 preserving the knot. In any case, the reader is warned that complex conjugation of the chart maps or the holonomy representation (see bellow) are not related to structures on manifolds with opposite orientation as in the case of real hyperbolic 3-manifolds.

On the other hand, it is not clear if a manifold (which has no orientation-reversing diffeomorphism) having a spherical CR structure will have another one inducing its opposite orientation. At least, if both orientations are induced

by spherical CR structures, then they are certainly very different as the induced contact structures themselves cannot be equivalent.

As with all geometric structures, a spherical structure on a manifold M induces a developing map defined on its universal cover $\tilde{M}$

$$d : \tilde{M} \to S^3$$

and a holonomy representation

$$\rho : \pi_1(M) \to \mathbf{PU}(2,1).$$

Observe again that precomposition with a diffeomorphism will induce an equivalent structure with a holonomy representation that is obtained from the old one by precomposition with an automorphism of the fundamental group. Also observe that the holonomy representation is not discrete in general and the developing map might be surjective. Surjectivity occurs frequently when one obtains new manifolds from connected sums of manifolds (see [5] for examples).

2.5. Branched Structures

Given a representation $\rho : \pi_1(M) \to \mathbf{PU}(2,1)$, it is not clear that it occurs as the holonomy representation of a spherical CR structure. In that sense, it is useful to introduce a more general definition of a branched structure in the hope that any given representation might be understood in a geometric way.

A branched spherical CR structure is a CR structure except along some curves where the structure is locally modeled on the t-axis inside $\mathbb{R}^3 = \{(z,t) \mid z \in \mathbb{C}, t \in \mathbb{R}\}$ together with the ramified map into the Heisenberg group given by

$$(z,t) \to (z^n, t),$$

where n is the branching order. The CR structure around the curve is given by the pullback of the CR structure around the Heisenberg t-axis.

As an example of a natural branched structure, consider the hypersurface $M \subset \mathbb{C}^2$ defined by

$$M = \{(z_1, z_2) \mid |z_1|^{2n} + |z_2|^2 = 1\}.$$

Observe then that the map $b : M \to S^3$ defined by $b(z_1, z_2) = (z_1^n, z_2)$ is branched along the $\mathbb{C}$-circle $z_2 = 0$.

We say that two branched structures are equivalent if there exists a diffeomorphism (CR outside the branching loci) that is a bijection restricted to the branching loci and whose composition with the local ramification maps around the branching loci also are local ramification maps.

3. The Figure-Eight Knot

We use some notation from the paper [4] and briefly recall the three irreducible representations obtained there.

The figure-eight knot complement M has a fundamental group $\Gamma = \pi_1(M)$ that can be presented as

$$\Gamma = \langle g_1, g_3 \mid [g_3, g_1^{-1}]g_3 = g_1[g_3, g_1^{-1}] \rangle.$$

It is useful to introduce the other generator

$$g_2 = [g_3, g_1^{-1}],$$

so that the relation in the presentation becomes

$$g_1 = g_2 g_3 g_2^{-1}.$$

The figure-eight knot complement is fibered over the circle with fiber a punctured torus. The fibration is encoded in the sequence

$$1 \to F_2 \to \Gamma \to \mathbb{Z} \to 0.$$

Here, F_2 is the free group of rank 2 with generators

$$F_2 = \langle a = g_2, b = [g_2, g_3^{-1}] \rangle.$$

We can then present

$$\Gamma = \langle a, b, t \mid tat^{-1} = aba, tbt^{-1} = ab \rangle,$$

where $t = g_3$ is seen to act as a pseudo-Anosov element of the mapping class group of the torus group.

We consider in this paper the following representations into $\mathbf{SU}(2, 1)$ obtained in [4]:

(1)

$$\rho_1(g_1) = \begin{pmatrix} 1 & 1 & -\frac{1}{2} - \frac{\sqrt{3}}{2}i \\ 0 & 1 & -1 \\ 0 & 0 & 1 \end{pmatrix}, \qquad \rho_1(g_3) = \begin{pmatrix} 1 & 0 & 0 \\ 1 & 1 & 0 \\ -\frac{1}{2} - \frac{\sqrt{3}}{2}i & -1 & 1 \end{pmatrix}.$$

(2)

$$\rho_2(g_1) = \begin{pmatrix} 1 & 1 & -\frac{1}{2} - \frac{\sqrt{7}}{2}i \\ 0 & 1 & -1 \\ 0 & 0 & 1 \end{pmatrix}, \qquad \rho_2(g_3) = \begin{pmatrix} 1 & 0 & 0 \\ -1 & 1 & 0 \\ -\frac{1}{2} + \frac{\sqrt{7}}{2}i & 1 & 1 \end{pmatrix}.$$

(3)

$$\rho_3(g_1) = \begin{pmatrix} 1 & 1 & -1/2 \\ 0 & 1 & -1 \\ 0 & 0 & 1 \end{pmatrix}, \qquad \rho_3(g_3) = \begin{pmatrix} 1 & 0 & 0 \\ \frac{5}{4} - \frac{\sqrt{7}}{4}i & 1 & 0 \\ -1 & -\frac{5}{4} - \frac{\sqrt{7}}{4}i & 1 \end{pmatrix}.$$

It turns out that the representation ρ_3 is obtained by precomposition of ρ_2 with the automorphisms of the fundamental group associated with a reversing orientation diffeomorphism (see [3] for a proof). We therefore concentrate on the first two representations during the rest of this paper.

4. Representations

As every complement of a tame knot, the complement of the figure-eight knot has fundamental group Γ fits in an exact sequence

$$1 \to [\Gamma, \Gamma] \to \Gamma \to \mathbb{Z} \to 0.$$

In the case of the complement of the figure-eight knot, we have

$$1 \to F_2 \to \Gamma \to \mathbb{Z} \to 0,$$

where F_2 is the free group of rank two. We will be interested in the general case where

$$1 \to F \to \Gamma \to \mathbb{Z} \to 0$$

is an exact sequence. Suppose that

$$\rho : \Gamma \to G$$

is a representation with $K = \mathrm{Ker}(\rho)$.

LEMMA 1. *The following diagram is commutative*:

$$\begin{array}{ccccccccc}
 & & 1 & & 1 & & 1 & & \\
 & & \downarrow & & \downarrow & & \downarrow & & \\
1 & \longrightarrow & K \cap F & \longrightarrow & K & \xrightarrow{\pi} & \pi(K) & \longrightarrow & 0 \\
 & & \downarrow & & \downarrow & & \downarrow & & \\
1 & \longrightarrow & F & \longrightarrow & \Gamma & \xrightarrow{\pi} & \mathbb{Z} & \longrightarrow & 0 \\
 & & \rho\downarrow & & \rho\downarrow & & \bar{\rho}\downarrow & & \\
1 & \longrightarrow & \rho(F) & \longrightarrow & \rho(\Gamma) & \xrightarrow{\bar{\pi}} & \rho(\Gamma)/\rho(F) & \longrightarrow & 0 \\
 & & \downarrow & & \downarrow & & \downarrow & & \\
 & & 1 & & 1 & & 1 & &
\end{array}$$

where $\bar{\pi}$ is the quotient map, and $\bar{\rho}$ is defined on a generator of $\mathbb{Z}$ as the image of a lift of a generator of $\mathbb{Z}$ (to Γ) under $\bar{\pi} \circ \rho$.

Proof. Clearly, $\bar{\rho}$ is well defined and makes the lower right corner of the diagram commutative. The only other verification we have to make is that $\mathrm{Ker}(\bar{\rho})$ is the image of $\pi(K)$. Suppose that $x = \pi(ft^n) \in \mathrm{Ker}(\bar{\rho})$ with $t \in \pi^{-1}(1)$, $n \in \mathbb{Z}$, and $f \in F$ satisfying

$$\bar{\pi}\rho(ft^n) = Id.$$

Then $\rho(ft^n) = \rho(f')$ with $f' \in F$. Therefore, $f'^{-1}ft^n \in K$, and then $x = \pi(ft^n) = \pi(f'^{-1}ft^n) \in \pi(K)$. □

We conclude that the inclusion $\rho(F) \subset \rho(\Gamma)$ has finite index if and only if K contains an element $ft^n, n \neq 0$, where $f \in F$ and $\pi(t) = 1$. The index is precisely the smallest absolute value of an integer satisfying the condition.

COROLLARY 2. *The inclusion $\rho(F) \lhd \rho(\Gamma)$ has infinite index if and only if $K \subset F$.*

4.1. The Representation ρ_1

In this section, we start reviewing some results of [4], in particular, the first two lemmas.

We consider the first representation. Let $\omega_3 = -\frac{1}{2} + i\frac{\sqrt{3}}{2}$. The ring of integers of the field $Q(i\sqrt{3})$ is $\mathcal{O}_3 = \mathbb{Z}[\omega_3]$. The representation is discrete since the generators G_1, G_2, G_3 are contained in the arithmetic lattice $P_3 = \mathbf{PU}(2, 1; \mathcal{O}_3)$.

We use the presentation of P_3 obtained in [6]:

$$P_3 = \langle P, Q, I \mid I^2 = (QP^{-1})^6 = PQ^{-1}IQP^{-1}I = P^3Q^{-2} = (IP)^3 \rangle.$$

Recall from [4] that $\rho_1(\Gamma)$ is generated by

$$G_1 = [P, Q],$$
$$G_2 = [I, [Q, P]],$$
$$G_3 = A[P, Q]A^{-1},$$

with $A = P^{-2}IP^2$.

A useful tool in the following computations is the normal subgroup $N = N(\rho_1(\Gamma)) \subset P_3$, the least normal subgroup of P_3 containing $\rho_1(\Gamma)$.

LEMMA 3. *P_3/N is isomorphic to $\mathbb{Z}/6\mathbb{Z}$.*

Computing that $P_3/[P_3, P_3]$ has order 6 and observing that $[P_3, P_3] \subset N$, we note that $N = [P_3, P_3]$. By computing the quotient of P_3 by the normalizer of $\langle G_1, I, [Q, P^{-1}] \rangle$ in P_3 we obtain the following:

LEMMA 4. $N = \langle G_1, I, [Q, P^{-1}] \rangle$.

LEMMA 5. *$P_3/[N, N]$ is isomorphic to the Euclidean triangle group of type $(2, 3, 6)$.*

Proof. Using the presentation of P_3 and Lemma 4, for the presentation of the quotient, we obtain

$$P_3/[N, N] = \langle P, Q \mid (QP^{-1})^6 = P^3 = Q^2 \rangle. \qquad \square$$

LEMMA 6. *$N/[N, N]$ is isomorphic to $\mathbb{Z} \oplus \mathbb{Z}$.*

Proof. From the isomorphism theorem

$$N/[N, N] = \frac{P_3/[N, N]}{P_3/N}$$

and from the two previous lemmas we obtain the result. $\square$

We have (cf. [4])

$$[\rho_1(\Gamma), \rho_1(\Gamma)] \lhd \rho_1(\Gamma) \lhd \langle G_1, I \rangle \lhd N \lhd \mathbf{PU}(2, 1; \mathcal{O}_3)$$

with the last inclusion of index 6 and the inclusion $\rho_1(\Gamma) \lhd \langle G_1, I\rangle$ of index at most two.

Observe now that the inclusion $\langle G_1, I\rangle \lhd N$ has abelian quotient and therefore $[N, N] \subset \langle G_1, I\rangle$, so we obtain

$$[\rho_1(\Gamma), \rho_1(\Gamma)] \subset [N, N] \lhd \langle G_1, I\rangle \lhd N \lhd \mathbf{PU}(2, 1; \mathcal{O}_3).$$

The following proposition was obtained after discussions with A. Reid. The proof given here is a simplification of his argument, which involved a GAP computation [11].

PROPOSITION 4.1. *The inclusions*

$$[\rho_1(\Gamma), \rho_1(\Gamma)] \lhd \rho_1(\Gamma) \subset \mathbf{PU}(2, 1; \mathcal{O}_3)$$

are of infinite index.

Proof. Observe first that $[\rho_1(\Gamma), \rho_1(\Gamma)] \lhd \langle G_1, I\rangle$ and $[N, N] \lhd \langle G_1, I\rangle$ are two normal inclusions and therefore

$$\langle G_1, I\rangle/[N, N] \to \langle G_1, I\rangle/[\rho_1(\Gamma), \rho_1(\Gamma)]$$

is a monomorphism. On the other hand, the quotient $\langle G_1, I\rangle/[\rho_1(\Gamma), \rho_1(\Gamma)]$ is finite or contains $\mathbb{Z}$ as a subgroup of index at most two.

Suppose now that $\rho_1(\Gamma) \subset \mathbf{PU}(2, 1; \mathbb{Z}[\omega])$ has finite index. Then $\langle G_1, I\rangle \lhd N$ should be of finite index, and therefore, since $N/[N, N] = \mathbb{Z} \oplus \mathbb{Z}$, we have $\langle G_1, I\rangle/[N, N] = \mathbb{Z} \oplus \mathbb{Z}$. This contradicts the fact that the above is a monomorphism.

Suppose next that $[\rho_1(\Gamma), \rho_1(\Gamma)] \lhd \rho_1(\Gamma)$ has finite index. Then the inclusion $[\rho_1(\Gamma), \rho_1(\Gamma)] \lhd \langle G_1, I\rangle$ would be of finite index. This, in turn, implies that $[N, N] \lhd \langle G_1, I\rangle$ has finite index. Since $N/\langle G_1, I\rangle$ is abelian of rank at most one, this contradicts the fact that $N/[N, N]$ is of rank two. □

From Lemma 1 and Proposition 4.1 we obtain the following:

COROLLARY 7.

$$\mathrm{Ker}(\rho_1) \lhd [\Gamma, \Gamma].$$

We conclude with the following property of the kernel:

PROPOSITION 4.2. $\mathrm{Ker}(\rho_1)$ *is not finitely generated.*

Proof. Observe that $\mathrm{Ker}(\rho_1)$ is clearly preserved under the pseudo-Anosov element of the mapping class group denoted by t. The result then follows from Lemma 6.2.5 in [9]. □

4.2. The Representation ρ_2

The second representation (see Section 6.5.1 in [4]) is given by $\Gamma_2 = \rho_2(\pi_1(M))$, with $\Gamma_2 = \langle \rho_2(g_1), \rho_2(g_2), \rho_2(g_3)\rangle$, where

$$G_1 := \rho_2(g_1) = \begin{pmatrix} 1 & 1 & -\frac{1}{2} - i\frac{\sqrt{7}}{2} \\ 0 & 1 & -1 \\ 0 & 0 & 1 \end{pmatrix},$$

$$G_2 := \rho_2(g_2) = \begin{pmatrix} 2 & \frac{3}{2} - i\frac{\sqrt{7}}{2} & -1 \\ -\frac{3}{2} - i\frac{\sqrt{7}}{2} & -1 & 0 \\ -1 & 0 & 0 \end{pmatrix},$$

$$G_3 := \rho_2(g_3) = \begin{pmatrix} 1 & 0 & 0 \\ -1 & 1 & 0 \\ -\frac{1}{2} + i\frac{\sqrt{7}}{2} & 1 & 1 \end{pmatrix}.$$

Moreover, $G_2 = [G_3, G_1^{-1}]$ is a regular elliptic element of order four, and G_1, G_3 are unipotent elements (also called pure parabolic elements).

REMARK 4.1. A simple computation shows that the element $G_3 G_1^{-1}$ is loxodromic. The fixed points of G_1, G_3 are respectively $p_1 = \infty$ and $p_2 = (0, 0)$.

Let $\omega_7 = \frac{1}{2} + i\frac{\sqrt{7}}{2}$. The ring of integers of the field $Q(i\sqrt{7})$ is $\mathcal{O}_7 = \mathbb{Z}[\omega_7]$. We observe then that the representation is discrete, since the generators G_1, G_2, G_3 are contained in the arithmetic lattice $\mathbf{PU}(2, 1; \mathcal{O}_7)$.

THEOREM 8 (see Proposition 3.3 and Theorem 4.4 in [13]). *The group* $\mathbf{PU}(2, 1; \mathcal{O}_7)$ *is generated by the elements*

$$I = \begin{pmatrix} 0 & 0 & 1 \\ 0 & -1 & 0 \\ 1 & 0 & 0 \end{pmatrix}, \quad R_1 = \begin{pmatrix} 1 & 0 & 0 \\ 0 & -1 & 0 \\ 0 & 0 & 1 \end{pmatrix}, \quad R_2 = \begin{pmatrix} 1 & 1 & -\bar{\omega}_7 \\ 0 & -1 & 1 \\ 0 & 0 & 1 \end{pmatrix},$$

$$R_3 = \begin{pmatrix} 1 & \bar{\omega}_7 & -1 \\ 0 & -1 & \omega_7 \\ 0 & 0 & 1 \end{pmatrix}, \qquad T = \begin{pmatrix} 1 & 0 & i\sqrt{7} \\ 0 & 1 & 0 \\ 0 & 0 & 1 \end{pmatrix}.$$

Moreover, the stabilizer subgroup of infinity has the presentation

$$\langle R_1, R_2, R_3, T \,|\, R_1^2 = R_3^2 = [T, R_1] = [T, R_3] = T R_2^{-2} = (R_1 R_3 R_2)^2 = Id \rangle.$$

We may express the generators of $\rho_2(\Gamma)$ in terms of the generators of $\mathbf{PU}(2, 1; \mathcal{O}_7)$:

PROPOSITION 4.3. *The following holds.*

$$G_1 = R_1 R_2 T^{-1} = R_1 R_2^{-1},$$
$$-G_2 = R_2 R_1 R_3 I,$$
$$G_3 = I R_2 I R_1 = I R_2 R_1 I = I G_1^{-1} I.$$

We also observe that

$$\rho_2(\Gamma) = \langle G_1, G_2, G_3\rangle = \langle G_1, G_3\rangle \lhd \langle G_1, I\rangle,$$

where $\langle G_1, G_3\rangle \lhd \langle G_1, I\rangle$ is a subgroup of index at most two since $G_3 = IG_1^{-1}I$.

We also have the following:

LEMMA 9. *We have*

$$\langle G_1, I, T\rangle \lhd \langle G_1, I, T, R_1\rangle = \mathbf{PU}(2, 1; \mathcal{O}_7).$$

Proof. $\langle G_1, I, T\rangle \lhd \langle G_1, I, T, R_1\rangle$ is a normal subgroup since $R_1G_1R_1 = T^{-1}G_1^{-1}$, $R_1IR_1 = I$, and $R_1TR_1 = T$. The normal inclusion is of index at most two. □

REMARK. The inclusion

$$\langle G_1, I\rangle \subset \langle G_1, I, T\rangle$$

can be neither normal nor finite if we prove that the limit set is not S^3. This is indeed the case by [3].

A simple computation shows the following:

LEMMA 10. *We have*

$$\rho_2(t^3) = [\rho_2(a^{-1}), \rho_2(b^{-1})].$$

From this lemma and from Lemma 2 we obtain the following:

COROLLARY 11. *The inclusion*

$$[\rho_2(\Gamma), \rho_2(\Gamma)] \lhd \rho_2(\Gamma)$$

is of index at most three.

5. Tetrahedra

5.1. Edges

Given two points p_1 and p_2 in S^3, there exists a unique $\mathbb{C}$-circle between them. Since the boundary of a complex disc has a positive orientation, the $\mathbb{C}$-circle inherits that orientation and defines therefore two distinct arcs $[p_1, p_2]$ and $[p_2, p_1]$ (see Figure 1). We will consider in this paper the edges that are one of the two arcs of a $\mathbb{C}$-circle.

We will need a construction of a disc in S^3 whose boundary is a given $\mathbb{C}$-circle. Although there is no preferred construction, we will obtain a disc as the union of $\mathbb{C}$-circles passing through a fixed point in the $\mathbb{C}$-circle (as in Figure 2). In the Heisenberg group model, if the fixed point is at infinity and the $\mathbb{C}$-circle is the vertical axis, then a simple choice of that disc is the union of vertical lines along the positive x-axis.

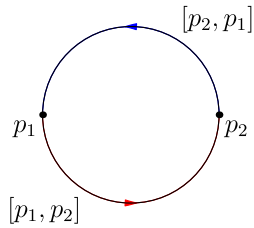

Figure 1 A $\mathbb{C}$-circle between two points in S^3 is oriented and defines two oriented segments

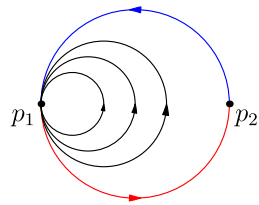

Figure 2 A disc foliated by $\mathbb{C}$-circles in S^3 whose boundary is a given $\mathbb{C}$-circle passing through two points

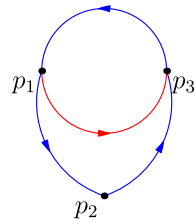

Figure 3 Triangles. We show four possible edges given a configuration of three points

5.2. Triangles

We suppose that we are given three points p_1, p_2, $p_3 \in S^3$ in general position (i.e., they do not belong to the same $\mathbb{C}$-circle). One can define an edge for each pair of points by choosing arcs of $\mathbb{C}$-circles as above. There is therefore a total of six choices for a 1-skeleton defining a triangle. Figure 3 shows two possible choices for the 1-skeleton.

Because we are on S^3, if we fix the 1-skeleton of a triangle, then we can clearly define (in many different ways) a 2-simplex with boundary defined by that 1-skeleton.

Perhaps the simplest example of a construction of a 2-simplex can be obtained fixing an ordering of the vertices of the triangle. Indeed, fix one point, say p_1, and consider the segments of $\mathbb{C}$-circles joining p_1 to the points of the edge $[p_2, p_3]$.

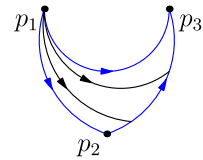

Figure 4 A triangle foliated by arcs in $\mathbb{C}$-circles. Given the ordered set (p_1, p_2, p_3), we choose the first point p_1 as the source of segments of $\mathbb{C}$-circles finishing at the segment $[p_2, p_3]$

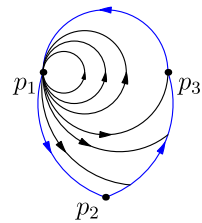

Figure 5 A triangle foliated by arcs in $\mathbb{C}$-circles. The triangle in this case is the union of the triangle in the previous figure and a disc whose boundary is the $\mathbb{C}$-circle containing p_1 and p_3

Figure 4 shows a 2-simplex formed using this procedure. It is easy to convince oneself that the union of segments obtained is actually a 2-simplex by fixing p_1 to be infinity in the Heisenberg model so that the 2-simplex is half a cylinder with base a finite $\mathbb{C}$-circle (i.e., an ellipse in the Heisenberg space).

If the edge $[p_1, p_3]$ were chosen differently (instead of the canonical procedure based on an order of the points described in the previous paragraph) to be the other half of the $\mathbb{C}$-circle, then one can add a disc as shown in Figure 5 in order to obtain a 2-simplex.

5.3. CR Tetrahedra

A 3-simplex based on a configuration of four points can be defined by a choice of a 2-simplex for each of the four configurations of three points. The problem is that the choices have to be compatible and faces, even if they are well defined, could intersect each other.

Given four points, each of the four triples of points defines canonical choices for faces up to a choice of order between the points (as explained in the previous section). But these canonical choices might not work, and, in that case, we have to try subdivisions: introducing auxiliary points so that the face will be a union of triangles.

Branched structures will be obtained by carefully constructing tetrahedra. The main problem will be to show that the faces are compatible and intersect only at common edges.

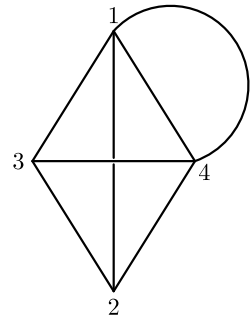

Figure 6 A tetrahedron with a disc adjoined to an edge

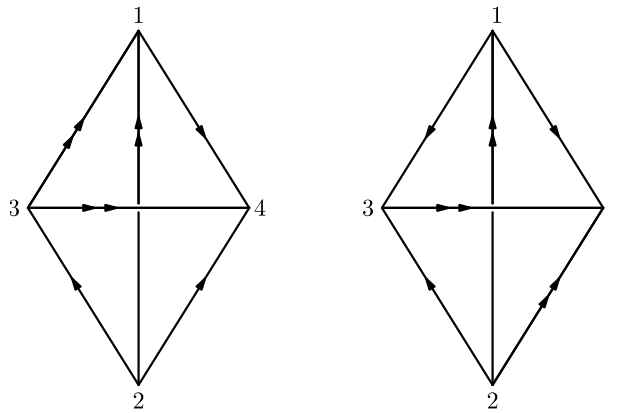

Figure 7 The figure eight knot complement represented by two tetrahedra with face pairings defined by the set of arrows

Sometimes we will deal with tetrahedra with discs adjoined to edges as in Figure 6.

DEFINITION 5.1. A 3-simplex with a disc adjoined to an edge is called a generalized tetrahedron.

That is a 3-simplex union a disc whose intersection with the simplex is an edge contained in the boundary of the disc.

6. Branched CR Structures Associated to Representations

In this section, we define the branched structure on the complement of the figure-eight knot. We leave the proof of some technical lemmas to the Appendix.

The representations in [4] are obtained by requiring that the 0-skeleton of an ideal triangulation defines a developing map. The triangulation of the figure-eight knot complement is shown in Figures 7 and 9. The 0-skeleton can be realized as

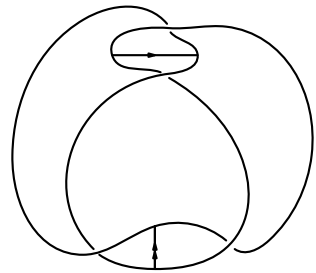

Figure 8 The figure-eight knot complement showing the two edges of the tetrahedra as two segments with end points in the knot. The ramification of the structure is along the edge with two arrows

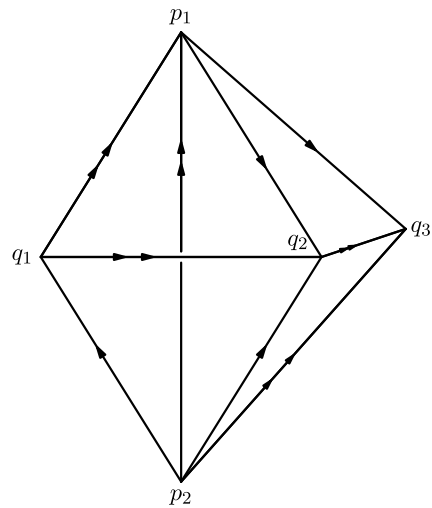

Figure 9 A schematic view of the two tetrahedra glued along one face

points in S^3, and using the side pairing maps, we can define a developing map on the 0-skeleton of the universal covering.

In order to obtain a spherical CR structure, we have to define the 1-skeleton and 2-skeleton and then obtain 3-simplices and show that the developing map defined on the 0-skeleton extends to the 3-simplices.

Once we obtain two 3-simplices in S^3 that have well-defined side pairings, we might have some branching along the edges of the simplices. In fact, we will prove that around one of the edges, the simplices are put together as in Figure 10, but along the other edge, we show that the six tetrahedra turn around the edge three times.

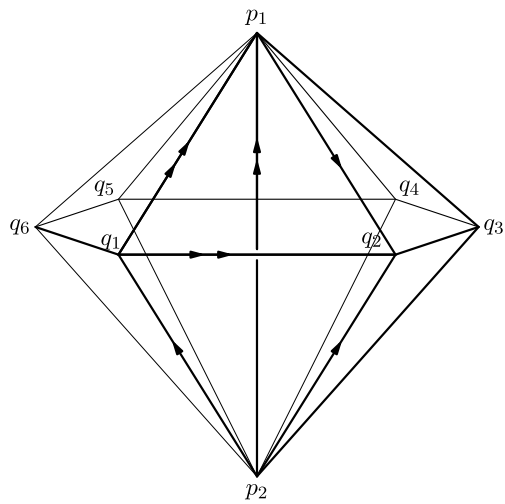

Figure 10 A schematic view of the six tetrahedra glued around the edge $[p_1, p_2]$

We therefore obtain a structure that is branched along one of the edges of the triangulation, namely, the edge with double arrows. The structure on the complement of the branching locus is a structure on the complement of a bouquet of two unknotted circles. Indeed, we can easily homotopy the complement of the knot union the branching locus in Figure 8 to two unknotted circles with one point in common.

Our main theorem is the following:

THEOREM 12. *The representation ρ_2 is discrete and is the holonomy of a branched spherical CR structure on the complement of the figure-eight knot.*

The discreteness of the representation follows from the observation that $\rho_2(\Gamma)$ is contained in a lattice. To prove the existence of a spherical CR structure on the complement of the figure-eight knot, it suffices to construct two tetrahedra in the Heisenberg space with side pairings that allow the definition of a developing map.

The rest of this section will be devoted to the construction of the two tetrahedra in the Heisenberg space and to verify the conditions so that the developing map is well defined. We define in Section 6.1 the 0-skeleton and the generators of the group that are defined by pairings of triples of vertices in the 0-skeleton (following [4]). In the next Section 6.2, we define the 1-skeleton by using segments of $\mathbb{C}$-circles. In Section 6.3, we define the 2-skeleton.

In the following sections, we prove the more technical results of the paper. Namely, we verify that the intersections of the faces are contained in the 1-skeleton, that the definition is compatible with the face pairings, and, finally, that around each of the two edges of the quotient manifold, the six tetrahedra around them define a branched structure.

We use half of a $\mathbb{C}$-circle to construct the segment between two given points. Recall that the $\mathbb{C}$-circle is oriented and, therefore, an oriented segment between two points corresponds to exactly one half of a $\mathbb{C}$-circle as explained in Section 5.1. For a given pair of points p and q in the Heisenberg space, we use $[p, q]$ to denote the segment connecting the two points with the direction from p to q.

6.1. The 0-Skeleton and the Side Pairings

We refer to Figure 10, where the tetrahedra around one edge (namely, $[p_2, p_1]$) are shown. The two tetrahedra are $T_1 := [p_1, p_2, q_1, q_2]$ and $T_2 := [p_1, p_2, q_2, q_3]$, where

$$p_1 = \infty, \quad p_2 = (0, 0), \quad q_1 = \left(1, \sqrt{7}\right),$$
$$q_2 = \left(\frac{5}{4} + i\frac{\sqrt{7}}{4}, 0\right), \qquad q_3 = \left(\frac{1}{4} + i\frac{\sqrt{7}}{4}, -\frac{\sqrt{7}}{2}\right).$$

The side paring transformations are

$$g_1 : (q_2, q_1, p_1) \to (q_3, p_2, p_1),$$
$$g_2 : (p_2, q_1, q_2) \to (p_1, q_2, q_3),$$
$$g_3 : (q_1, p_2, p_1) \to (q_2, p_2, q_3).$$

There are six tetrahedra around the edge $[p_2, p_1]$ (see Figure 10) and $[p_2, q_2]$, respectively. They are obtained by translating T_1 and T_2. They are

$$T_1, T_2, G_1(T_1), G_1G_3^{-1}(T_2), G_1G_3^{-1}G_2(T_1), G_1G_3^{-1}G_2G_1^{-1}(T_2),$$

and respectively

$$T_1, T_2, G_3(T_1), G_3G_2^{-1}(T_2), G_3G_2^{-1}(T_1), G_3G_2^{-1}G_1^{-1}(T_2).$$

Following the side parings, it is easy to compute the following (where we define the points q_4, q_5, q_6):

(1) $G_1(q_2, q_1, p_1) = (q_3, p_2, p_1)$.
(2) $G_1G_3^{-1}(q_2, p_2, q_3) = (p_2, q_4, p_1)$ with

$$q_4 = G_1(p_2) = \left(-1, -\sqrt{7}\right).$$

(3) $G_1G_3^{-1}G_2(p_2, q_1, q_2) = (q_5, p_2, p_1)$ with

$$q_5 = G_1G_3^{-1}(p_1) = \left(\frac{-5}{4} + i\frac{\sqrt{7}}{4}, 0\right).$$

(4) $G_1G_3^{-1}G_2G_1^{-1}(q_3, p_2, p_1) = (p_1, p_2, q_6)$ with

$$q_6 = G_1G_3^{-1}G_2(p_1) = \left(-\frac{1}{4} + i\frac{\sqrt{7}}{4}, \frac{\sqrt{7}}{2}\right)$$

and $G_1G_3^{-1}G_2G_1^{-1}(q_2) = q_1$.
(5) Since $G_1G_3^{-1}G_2G_1^{-1}G_3(q_1, p_2, p_1) = (q_1, p_2, p_1)$, $G_1G_3^{-1}G_2G_1^{-1}G_3 = Id$.

We also compute the following (where we define the points p_3, p_4, p_5):

(1) $G_3(p_2, q_1, q_2) = (p_2, q_2, p_3)$ with

$$p_3 = G_3(q_2) = \left(\frac{23}{32} + i\frac{5\sqrt{7}}{32}, -\frac{\sqrt{7}}{16}\right).$$

(2) $G_3G_2^{-1}(p_1, p_2, q_2) = (p_2, p_4, q_2)$ with

$$p_4 = G_3G_2^{-1}(p_2) = \left(\frac{5}{8} + i\frac{\sqrt{7}}{8}, 0\right).$$

(3) $G_3G_2^{-1}(p_1, q_1, q_2) = (p_2, p_5, q_2)$ with

$$p_5 = G_3G_2^{-1}(q_1) = \left(\frac{3}{4} + i\frac{\sqrt{7}}{4}, 0\right).$$

(4) $G_3G_2^{-1}G_1^{-1}(p_1, q_2, q_3) = (p_2, q_1, q_2)$.
(5) Since $G_3G_2^{-1}G_1^{-1}G_2(p_2, q_1, q_2) = (p_2, q_1, q_2)$, $G_3G_2^{-1}G_1^{-1}G_2 = Id$.

6.2. The 1-Skeleton

In fact, considering the orientations of the edges, there are four possibilities for the choice of the 1-skeleton. Here, we consider one choice given in Figure 11. Precisely, $[p_2, p_1] = (0, t)$ with $t \leq 0$, and

$$[p_2, q_2] = \left(\frac{5 + i\sqrt{7}}{8} + \frac{\sqrt{2}}{2}e^{i\theta}, \frac{1}{8}\left(\sqrt{14}\cos(\theta) - 5\sqrt{2}\sin(\theta)\right)\right),$$

where $\theta \in [\arccos(\frac{5\sqrt{2}}{8}), 2\pi - \arccos(-\frac{5\sqrt{2}}{8})]$. The other edges are determined from these two by applying the side-pairings.

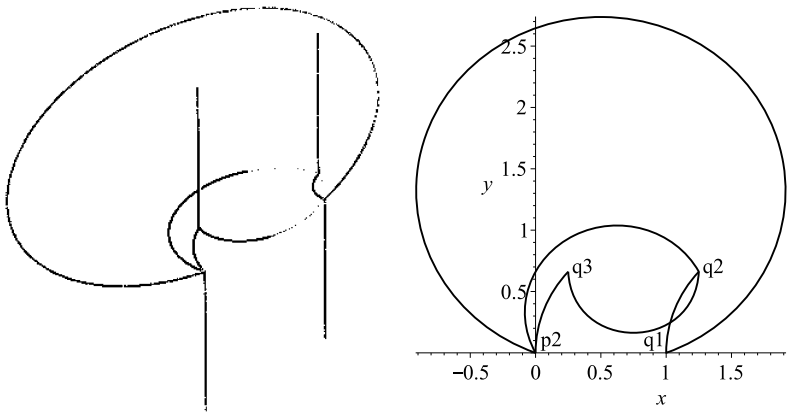

(a) The space view (b) The projected view

Figure 11 The 1-skeleton of the tetrahedra

6.3. The 2-Skeleton

In this subsection, we give the details of the construction of the faces of the two tetrahedra.

The basic construction of a triangle (a face of a tetrahedron) is described in Section 3. A canonical construction of the 2-skeleton only using the procedure described there (which depends on an order of three vertices defining a 2-simplex) does not work in that case; there are undesired intersections between faces of the tetrahedra that are not contained in the 1-skeleton.

We modify the procedure introducing an ad hoc division of the face. After this choice of division, the procedure is canonical, namely, for each smaller triangle in the face, we follow the canonical procedure. Unfortunately, the choice of the division (for instance, the definition of v_1, v_2, and v_3 in Figure 12) is not canonical but was guided by numerical experiments. On one hand, that makes the construction difficult to follow for the reader because it is ad hoc; on the other hand, it is very flexible, and we can quickly find what the faces should be by numerical computations on a computer.

6.3.1. Faces of T_1. We refer to Figure 12 for a schematic description of the four faces.

(1) $F(p_2, q_1, q_2)$: Choose $v_1 = (\frac{3}{2} + i\frac{\sqrt{7}}{2}, 0)$ to be the center of the triangle (p_2, q_1, q_2), then define $F(p_2, q_1, q_2)$ to be the union of triangles $F(v_1, q_1, q_2)$, $F(p_2, q_1, v_1)$, and $F(p_2, q_2, v_1)$.
   - $F(v_1, q_1, q_2)$ is the union of segments starting at v_1 and ending at the edge $[q_1, q_2]$;
   - $F(p_2, q_1, v_1)$ is the union of segments starting at p_2 and ending at the edge $[v_1, q_1]$;
   - $F(p_2, q_2, v_1)$ is the union of segments starting at p_2 and ending at the edge $[v_1, q_2]$.

(2) $F(p_1, p_2, q_1)$: Choose the point

$$v_2 = \left(\frac{1}{2} + i\left(\frac{\sqrt{7}}{2} + \sqrt{2}\right), -\sqrt{2}\right) \in [p_2, q_1]$$

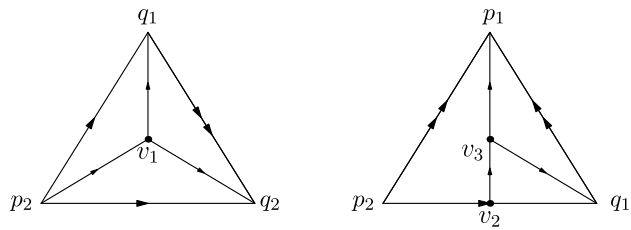

Figure 12 A schematic view of faces $F(p_2, q_1, q_2)$ (left) and $F(p_1, p_2, q_1)$ (right)

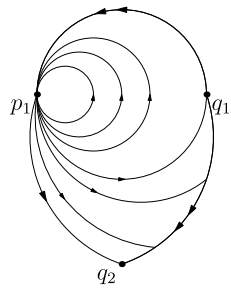

Figure 13 A schematic view of the face $F(p_1, q_1, q_2)$

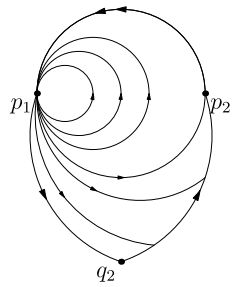

Figure 14 A schematic view of the face $F(p_1, p_2, q_2)$

and connect v_2 and p_1 by the edge $[v_2, p_1]$. Choose

$$v_3 = \left(\frac{1}{2} + i\left(\frac{\sqrt{7}}{2} + \sqrt{2}\right), -\sqrt{2} - 6\sqrt{2}\right) \in [v_2, p_1],$$

then the face $F(p_1, p_2, q_1)$ is the union of faces $F(q_1, v_2, v_3)$, $F(p_1, q_1, v_3)$, and $F(p_1, p_2, v_2)$.

- $F(p_1, p_2, v_2)$ is the union of segments starting at each point of the segment $[p_2, v_2]$ and ending at p_1;
- $F(q_1, v_2, v_3)$ is the union of segments starting at each point of the segment $[v_2, v_3]$ and ending at q_1;
- $F(p_1, q_1, v_3)$ is the union of segments starting at each point of the segment $[v_3, q_1]$ and ending at p_1.

(3) $F(p_1, q_1, q_2)$: It has two subfaces; one is a triangle face that is the union of segments from p_1 to the edge $[q_1, q_2]$; the other one is a disc that is the union of $\mathbb{C}$-circles passing through p_1 and the half-line $\{(1 + it, \sqrt{7}) : \ t \leq 0\}$. See Figure 13.

(4) $F(p_1, p_2, q_2)$: Its construction is similar to the face $F(p_1, q_1, q_2)$. It also has two subfaces; one is the union of segments from p_1 to the edge $[p_2, q_2]$, and the other is a disc that is the union of $\mathbb{C}$-circles passing through p_1 and the negative half of the y-axis in Heisenberg space. See Figure 14.

6.3.2. Faces of T_2. The faces of T_2 are all determined by the faces of T_1 by applying the side pairings.

(1) $F(p_1, q_2, q_3)$: Let

$$v_4 = G_2(v_1) = \left(\frac{3}{4} + i\frac{\sqrt{7}}{4}, 0\right).$$

Since $F(p_1, q_2, q_3) = G_2(F(p_2, q_1, q_2))$, $F(p_1, q_2, q_3)$ is the union of three faces, which are:

- $F(v_4, q_2, q_3)$ is the union of segments starting at v_4 and ending at the edge $[q_2, q_3]$;
- $F(p_1, v_4, q_2)$ is the union of the segments from p_1 to the segment $[v_4, q_2]$;
- $F(p_1, v_4, q_3)$ is the union of the segments from p_1 to the segment $[v_4, q_3]$.

(2) $F(q_3, p_2, q_2)$: Let

$$v_5 = G_3(v_2) \in [p_2, q_2].$$

Connect v_5 and q_3 by the edge $[v_5, q_3] = G_3([v_2, p_1])$ and let $v_6 = G_3(v_3) \in [v_5, q_3]$. Since $F(q_3, p_2, q_2) = G_3(F(p_1, p_2, q_1))$, the face $F(q_3, p_2, q_2)$ is the union of three faces, which are:

- $F(q_3, p_2, v_5)$ is the union of the segments from the segment $[p_2, v_5]$ to q_3;
- $F(q_2, v_5, v_6)$ is the union of the segments from the segment $[v_5, v_6]$ to q_2;
- $F(q_3, v_6, q_2)$ is the union of the segments from the segment $[v_6, q_2]$ to q_3.

(3) $F(p_1, p_2, q_2)$: It is the same as the definition of that face in the tetrahedron T_1.

(4) $F(p_1, p_2, q_3)$: From $F(p_1, p_2, q_3) = G_1(F(p_1, q_1, q_2))$ it is easy to see that the face $F(p_1, p_2, q_3)$ is the union of segments from p_1 to the edge $[p_2, q_3]$ and a disc that is the union of $\mathbb{C}$-circles passing through p_1 and the negative half of the y-axis.

6.4. The Tetrahedra

In this subsection, we want to show that the faces of the tetrahedra constructed above define two tetrahedra.

Following the construction of the 2-skeleton, it is easy to show that each face is embedded.

LEMMA 13. *Each face of the two tetrahedra defined in the above section is topologically a disc in the Heisenberg space.*

LEMMA 14. *The tetrahedron T_1 defined above is homeomorphic to a tetrahedron.*

LEMMA 15. *The tetrahedron T_2 defined above is homeomorphic to a generalized tetrahedron.*

LEMMA 16. $T_1 \cap T_2 = F(p_1, p_2, q_2)$.

From the definition of T_1 and T_2 and form the above lemmas we have the following:

LEMMA 17. *G_1, G_2, G_3 are side parings of the union $T_1 \cup T_2$.*

PROPOSITION 6.1. *The quotient space of $T_1 \cup T_2$-{vertices} under the side parings G_1, G_2, G_3 is the complement of the figure-eight knot.*

6.5. The Structure Around the Edges

The quotient of $T_1 \cup T_2$ by the side parings has two edges, represented by $[p_2, p_1]$ and $[p_2, q_2]$. The purpose of this subsection is to show that the neighborhood around those edges covers a neighborhood of half of the t-axis in the Heisenberg space. The phenomenon is similar to that in Subsection 6.4 of [4].

6.5.1. The Neighborhood Around $[p_2, p_1]$. We know that the neighborhood around $[p_2, p_1]$ is a union of neighborhoods contained in

$$\begin{aligned} T_1 &= [p_1, p_2, q_1, q_2], \\ T_2 &= [p_1, p_2, q_2, q_3], \\ T_3 &= G_1(T_1) = [p_1, q_4, p_2, q_3], \\ T_4 &= G_1 G_3^{-1}(T_2) = [q_5, q_4, p_2, p_1], \\ T_5 &= G_1 G_3^{-1} G_2(T_1) = [q_6, q_5, p_2, p_1], \end{aligned}$$

and

$$T_6 = G_1 G_3^{-1} G_2 G_1^{-1}(T_2) = [q_6, p_2, q_1, p_1].$$

From the above six tetrahedra we know that the six faces with the same edge $[p_2, p_1]$ are $F(p_2, p_1, q_j)$, where $j = 1, \ldots, 6$. By arguing as in [4] it is easy to see that each pair of consecutive tetrahedra T_j and T_{j+1} match along the matching face $F(p_2, p_1, q_{j+1})$.

Let N_j, $j = 1, \ldots, 6$, denote the neighborhoods along the edge $[p_2, p_1]$ contained in the six tetrahedra T_j. By analyzing the positions of those neighborhoods in the Heisenberg space (see Figure 15 for a schematic description) we have the following proposition.

PROPOSITION 6.2. *The union $\bigcup N_j$ forms a standard tubular neighborhood of $[p_2, p_1]$ in the Heisenberg space.*

6.5.2. The Neighborhood Around $[p_2, q_2]$. The neighborhood around $[p_2, q_2]$ is a union of neighborhoods contained in the six tetrahedra

$$\begin{aligned} T_1' &= T_1 = [p_1, p_2, q_1, q_2], \\ T_2' &= T_2 = [p_1, p_2, q_2, q_3], \\ T_3' &= G_3(T_1) = [q_3, p_2, q_2, p_3], \\ T_4' &= G_3 G_2^{-1}(T_2) = [p_2, p_4, q_2, p_3], \\ T_5' &= G_3 G_2^{-1}(T_1) = [p_2, p_4, p_5, q_2], \end{aligned}$$

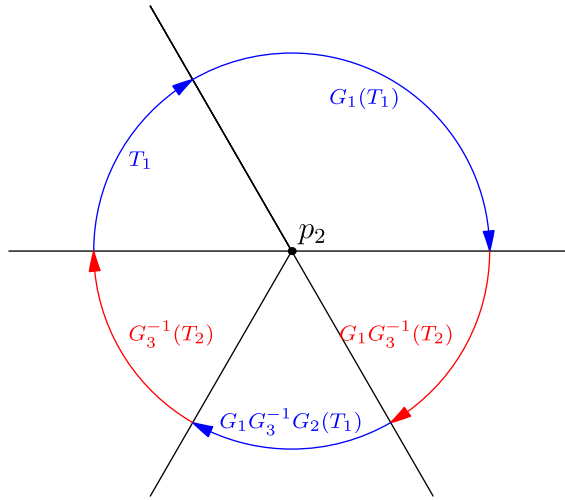

Figure 15 A schematic picture of a neighborhood around the edge $[p_1, p_2]$, where the segments stand for the faces with the common edge $[p_1, p_2]$ (denoted by the common intersection point p_2). The arcs and the regions between two segments stand for the neighborhoods contained in one tetrahedron

and

$$T_6' = G_3G_2^{-1}G_1^{-1}(T_2) = G_2^{-1}(T_2) = [p_2, p_5, q_1, q_2].$$

Let N_j', $j = 1, \ldots, 6$, denote neighborhoods along the edge $[p_2, q_2]$ contained in the corresponding tetrahedrons T_j'. We can determine the positions of those tetrahedra using their faces containing the edge $[p_2, q_2]$ and the intersections with a tubular neighborhood of $[p_2, q_2]$. (See Figure 16 for a schematic description of the position of the neighborhoods.) By a similar argument as in [4], we can conclude the following:

PROPOSITION 6.3. *The union* $\bigcup N_j'$ *forms a neighborhood covering three times a tubular neighborhood of the edge* $[p_2, q_2]$ *in the Heisenberg space.*

That is, the structure obtained by gluing tetrahedra around the edge $[p_2, q_2]$ is a ramified CR structure with index of ramification 3.

REMARK 6.1. We correct a statement in [4]. In fact, the union of the neighborhoods contained in the tetrahedra around the edge $[p_2, p_4]$ (in the case of the first representation discussed there) forms a neighborhood of this edge, and not a three times cover as announced in the paper. This implies that the structure constructed there is ramified along only one edge.

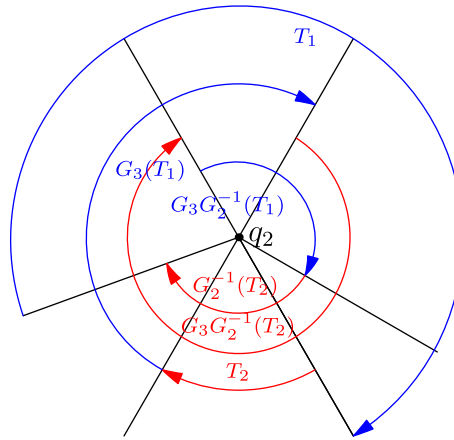

Figure 16 A schematic picture showing the neighborhoods corresponding to each tetrahedron. The segments stand for the faces with the common edge $[p_2, q_2]$ (which is represented by the point q_2), and the arcs and the region between two segments denote the neighborhoods contained in one tetrahedron

Appendix

In this section, we give proofs of some technical lemmas. In particular, we prove Lemmas 14–16 contained in Section 6.5.

Let $\Pi : \mathfrak{N} \to \mathbb{C}$ be the vertical projection map from the Heisenberg space onto the z-plane. When describing projections in this section, we will use the same notation for a point in the Heisenberg group and its projection in the z-plane.

A.1. Proof of Lemma 14

It suffices to show that each pair of faces only intersects at their common edge. It is well known that any $\mathbb{C}$-circle passing through the point at infinity is a vertical line in the Heisenberg space. Hence, any segment with p_1 as an endpoint will project to a point on the z-plane.

First, we analyze the projections on the z-plane of the projections of the faces of the tetrahedron T_1. It is easy to determine their projections (see Figure 17):

- $\Pi(F(p_1, p_2, q_2))$: The union of the (circle) curve p_2q_2 and the negative y-axis starting at p_2;
- $\Pi(F(p_1, q_1, q_2))$: The union of the (circle) curve q_1q_2 and the half-line parallel to the y-axis starting at q_1;
- $\Pi(F(p_1, p_2, q_1))$: The union of p_2v_2 and the region between the two curves connecting v_2 and q_1;
- $\Pi(F(p_2, q_1, q_2))$: The union of the triangles (p_2, v_1, q_2) and (v_1, q_1, q_2) and the curves from the point p_2 to the curve v_1q_1.

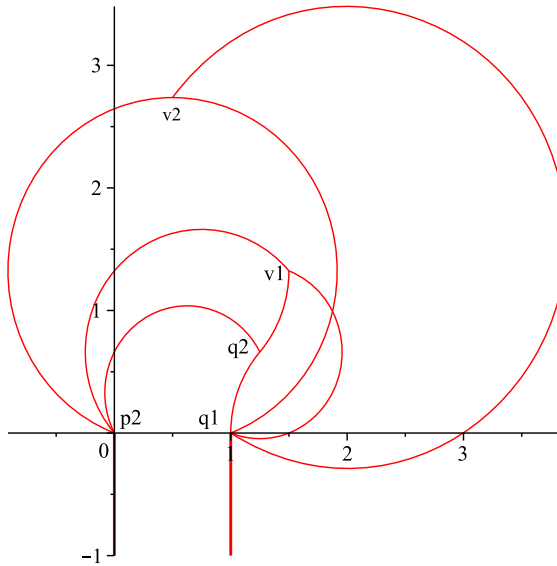

Figure 17 The projections of the faces of T_1

The only one we have to check carefully is

$$F(p_2, q_1, q_2) \cap F(p_1, p_2, q_1) = [p_2, q_1]$$

since the others obviously intersect at their common edge. Recall that both of the faces contain three subfaces, so it suffices to prove

$$F(p_2, q_1, v_1) \cap F(q_1, v_2, v_3) = [v_2, q_1]$$

since $v_2 \in [p_2, q_1]$. As it is not easy to see this from their projections, we consider the images of these two faces by the transformation G_2 that will transform the point p_2 to the point at infinity p_1:

$$\begin{aligned} G_2(F(p_2, q_1, v_1) \cap F(q_1, v_2, v_3)) &= G_2(F(p_2, q_1, v_1)) \cap G_2(F(q_1, v_2, v_3)) \\ &= F(p_1, q_2, v_4) \cap F(q_2, v_2', v_3'), \end{aligned}$$

where

$$v_2' = G_2(v_2) = \left(\frac{5}{4} + i\frac{\sqrt{7}}{4}, \sqrt{2}\right) \in G_2([p_2, q_1]) = [p_1, q_2]$$

and

$$\begin{aligned} v_3' = G_2(v_3) = &\left(\frac{40 + \sqrt{14}}{32 + 2\sqrt{14}} + i\frac{5\sqrt{2} + 14\sqrt{7}}{32 + 2\sqrt{14}}, -\frac{\sqrt{2} + 2\sqrt{7}}{32 + 2\sqrt{14}}\right) \\ &\in G_2([v_2, p_1]) = [v_2', v_1]. \end{aligned}$$

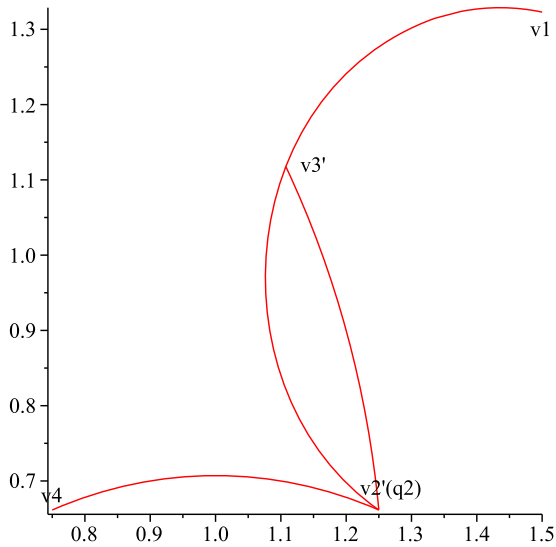

Figure 18 The projection $\Pi(F(p_1, q_2, v_4))$ is the curve v_4q_2, and $\Pi(F(q_2, v_2', v_3'))$ is the region bounded by the two curves connecting v_2' and v_3'

It can be seen that

$$F(p_1, q_2, v_4) \cap F(q_2, v_2', v_3') = [v_2', q_2] = G_2([v_2, q_1])$$

by analyzing their projections (see Figure 18), which completes our proof.

A.2. Proof of Lemma 15

As in the proof of the above lemma, we first consider the projections of the faces given in Figure 19:

- $\Pi(F(p_1, p_2, q_2))$: It is the union of the circle segment p_2q_2 and the negative half y-axis, which is the projection of the disc part;
- $\Pi(F(p_1, p_2, q_3))$: It is the union of the circle segment p_2q_3 and the negative half y-axis;
- $\Pi(F(p_1, q_2, q_3))$: It is the triangle (v_4, q_2, q_3);
- $\Pi(F(p_2, q_2, q_3))$: It is the union of $\Pi(F(p_2, v_5, q_3))$, $\Pi(F(v_6, q_2, q_3))$, and $\Pi(F(q_2, v_5, v_6))$, which is the union of (circle) curves from the point q_2 to the (circle) curve v_5v_6.

The intersections of each pair of faces are easily obtained, except

$$F(p_1, q_2, q_3) \cap F(p_2, q_2, q_3) = [q_2, q_3]$$

and

$$F(p_2, q_2, q_3) \cap F(p_2, q_2, p_1) = [p_2, q_2].$$

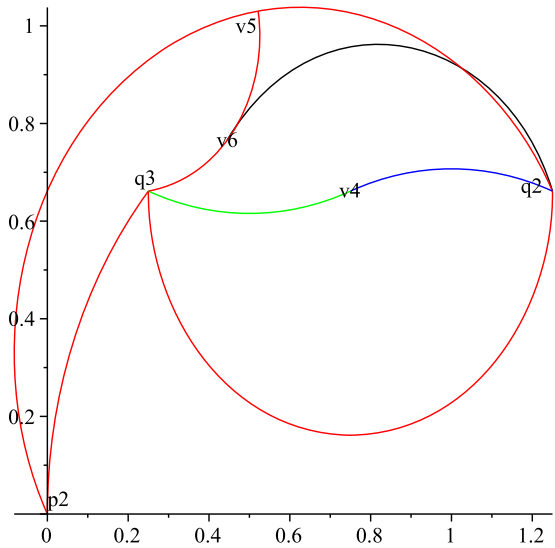

Figure 19 The projections of the faces of T_2

The first one can be obtained by considering their images under G_3^{-1}. We have to show

$$\begin{aligned} G_3^{-1}(F(p_1,q_2,q_3)\cap F(p_2,q_2,q_3)) &= G_3^{-1}(F(p_1,q_2,q_3))\cap G_3^{-1}(F(p_2,q_2,q_3)) \\ &= F(G_3^{-1}(p_1),q_1,p_1)\cap F(p_2,q_1,p_1) \\ &= [q_1,p_1] = G_3^{-1}([q_2,q_3]). \end{aligned}$$

Let

$$p_1' = G_3^{-1}(p_1) = \left(-\frac{1}{4}+i\frac{\sqrt{7}}{4},\frac{\sqrt{7}}{2}\right)$$

and

$$v_4' = G_3^{-1}(v_4) = \left(\frac{1}{2}+i\frac{\sqrt{7}}{2},0\right).$$

It suffices to show that

$$F(v_4',q_1,p_1)\cap F(q_1,v_2,p_1) = [q_1,p_1]$$

since the other two subfaces $F(p_1,v_4,q_2)$ and $F(p_1,v_4,q_3)$ of $F(p_1,q_2,q_3)$ do not intersect the face $F(p_2,q_2,q_3)$. This can be verified by analyzing their projections in Figure 20, where the projections of $F(v_4',q_1,p_1)$ lie in the region between the straight line and the circle segment with the same endpoints v_4' and q_1.

To prove

$$F(p_2,q_2,q_3)\cap F(p_2,q_2,p_1) = [p_2,q_2]$$

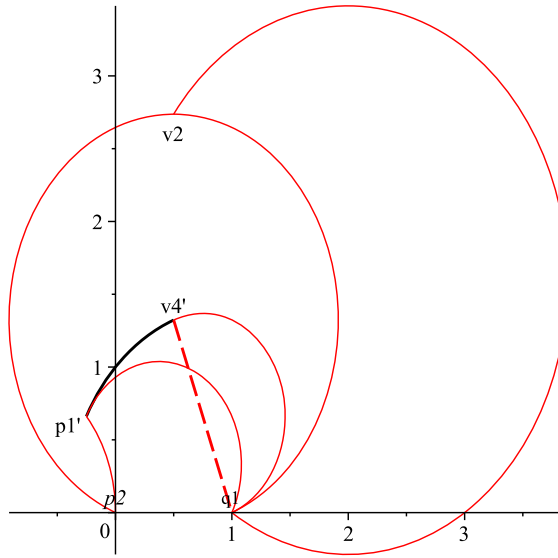

Figure 20 The projections of the faces $F(p_1', q_1, p_1)$, $F(p_2, q_1, p_1)$, and $F(p_2, q_1, p_1')$

is equivalent to show

$$G_3^{-1}(F(p_2, q_2, q_3)) \cap G_3^{-1}(F(p_2, q_2, p_1)) = F(p_2, q_1, p_1) \cap F(p_2, q_1, p_1') = [p_2, q_1].$$

The result is clear by analyzing the projections in Figure 20 since the projections of $F(p_2, q_1, p_1')$ lie in the triangle (p_1', p_2, q_1).

At last, we have to mention that the intersection of $F(p_1, p_2, q_2)$ and $F(p_1, p_2, q_3)$ is a disc, not only an edge (T_2 is a generalized tetrahedron).

A.3. Proof of Lemma 16

According to the projections of the faces of the two tetrahedra given in Figure 21, we only need to prove the following cases in detail.

- $F(p_1, q_1, q_2) \cap F(p_1, q_2, q_3) = [p_1, q_2]$. Recall that the face $F(p_1, q_2, q_3)$ has three parts. It is easy to see that

$$F(p_1, q_1, q_2) \cap F(p_1, q_2, v_4) = [p_1, q_2]$$

and

$$F(p_1, q_1, q_2) \cap F(p_1, v_4, q_3) = p_1.$$

Therefore, it suffices to show

$$F(v_4, q_2, q_3) \cap F(q_1, q_2, p_1) = q_2,$$

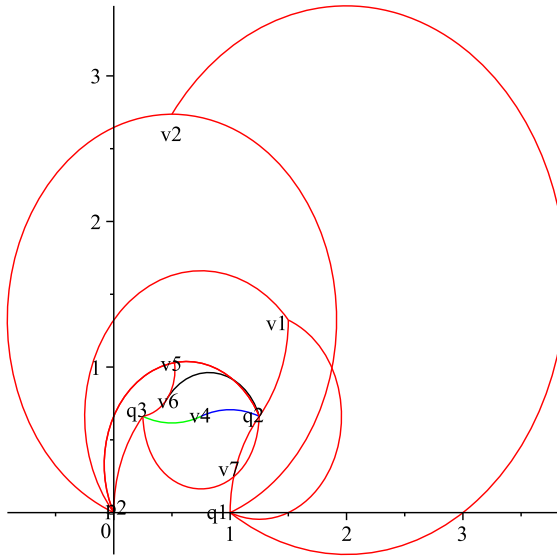

Figure 21 The projection of the subfaces of T_1 and T_2

which follows by comparing the height functions of the two faces. From their projections we only need to compare the height of the parts where they have intersected projections, that is, the segment $[v_7, q_2] \subset [q_1, q_2]$, where $v_7 = (\frac{33}{32} + i\frac{3\sqrt{7}}{32}, \frac{5\sqrt{7}}{8})$. More precisely, write the x and y coordinates of

$$[v_7, q_2] = \big(2 + e^{i\theta}, \sqrt{7} - 4\sin(\theta)\big),$$

where

$$\theta \in \left[\pi - \arcsin\left(\frac{\sqrt{7}}{4}\right), \pi - \arcsin\left(\frac{3\sqrt{7}}{32}\right)\right],$$

into the parameterization of the face

$$F(v_4, q_2, q_3) = \begin{cases} (x - x_0)^2 + (y - y_0)^2 = 1/2, \\ t = t_0 + 2(y_0 x - x_0 y), \end{cases}$$

where

$$\begin{cases} x_0 = (\cos(\varphi) + \sqrt{7}\sin(\varphi) + 3)/4, \\ y_0 = (-\sqrt{7}\cos(\varphi) + \sin(\varphi) + \sqrt{7})/4, \\ t_0 = (\sqrt{7}\cos(\varphi) + \sin(\varphi))/2, \end{cases}$$

with $\varphi \in [\pi, 2\pi]$, we can get the height function $t_1 = t_1(\theta)$ as a function of θ. Let $t_2 = \sqrt{7} - 4\sin(\theta)$; then we can compare these two height functions (see Figure 22) so that the height of $[v_7, q_2]$ is bigger than that in $F(v_4, q_2, q_3)$. This implies that $F(v_4, q_2, q_3)$ and $F(q_1, q_2, p_1)$ only intersect at the point q_2.

- $F(p_2, q_1, q_2) \cap F(p_2, q_2, q_3) = [p_2, q_2]$.
- $F(p_2, q_1, q_2) \cap F(p_1, q_2, q_3) = q_2$.

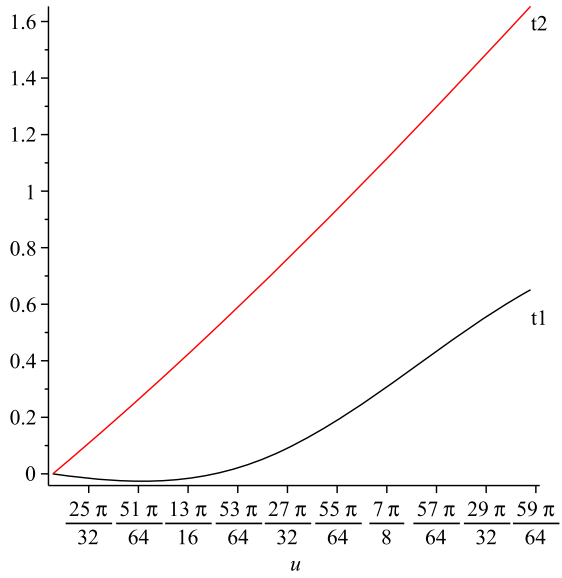

Figure 22 The height comparison, where t_1, t_2 denote the height in $[v_7, q_2]$ and $F(v_4, q_2, q_3)$, respectively

The last two can be proved by a similar argument as in the proof of Lemma 14 and Lemma 15. More precisely, we consider their images under the action of G_2. Recall that

$$G_2(F(p_2, q_1, q_2)) = F(p_1, q_2, q_3)$$

and $v_1 = G_2(p_1)$. Let $v_4' = G_2(q_3)$; then

$$G_2(F(p_1, q_2, q_3)) = F(v_1, q_3, v_4')$$

and

$$G_2(F(p_2, q_2, q_3)) = F(p_1, q_3, v_4').$$

Recall that each of these faces has three parts; according to the projected view in Figure 21, we only need to check the intersections of their subfaces

$$F(p_2, v_1, q_2) \cap F(v_5, v_6, q_2) = [v_5, q_2]$$

and

$$F(v_1, q_1, q_2) \cap F(v_4, q_2, q_3) = q_2.$$

These can be proved by analyzing the projections of their images by G_2 in Figure 23. Precisely, let

$$v_5' = G_2(v_5) = \left(\frac{1}{4} + i\frac{\sqrt{7}}{4}, \frac{\sqrt{2}}{8 + 2\sqrt{14}}\right),$$

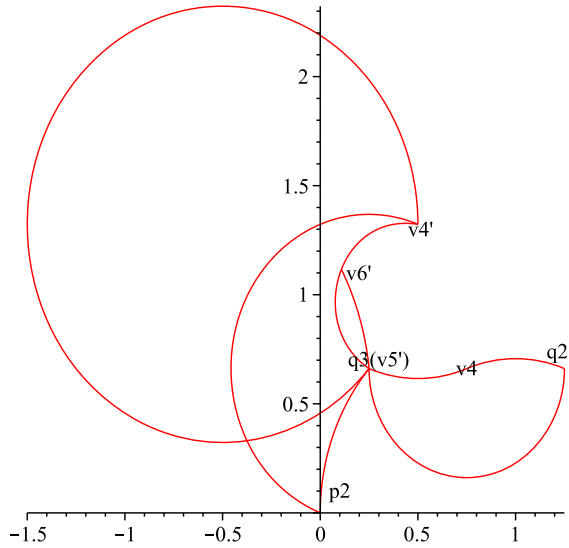

Figure 23 Projections of $F(p_1, q_2, q_3)$, $F(p_2, q_3, v_4')$, and $F(q_3, v_5', v_6')$

$$v_6' = G_2(v_6) = \left(\frac{8-\sqrt{14}}{32+2\sqrt{14}} + i\,\frac{5\sqrt{2}+14\sqrt{7}}{32+2\sqrt{14}}, -\frac{5\sqrt{2}+6\sqrt{7}}{32+2\sqrt{14}} \right)$$

and recall that $p_2 = G_2(v_4)$. Then their projections are:

- $\Pi(F(p_1, q_2, q_3))$ is the triangle (v_4, q_2, q_3);
- $\Pi(F(p_2, q_3, v_4'))$ is the union of (circle) curves from the curve p_2q_3 to the point v_4'. This projection is more complicated but lies outside the triangle (v_4, q_2, q_3);
- $\Pi(F(q_3, v_5', v_6'))$ is the region bounded by the two curves connecting the points v_5' and v_6'.

Observe that the points v_5' and q_3 denote the same points on the z-plane.

ACKNOWLEDGMENTS. We thank M. Deraux, A. Guilloux, A. Reid, P. Will, and M. Wolff for fruitful discussions. We also thank an anonymous referee for helping to improve the previous version of this paper. The second author is grateful to Université Pierre et Marie Curie for the hospitality and support. He also thanks Yueping Jiang, Baohua Xie, and Wenyuan Yang for their encouragements.

References

[1] D. Burns and S. Shnider, *Spherical hypersurfaces in complex manifolds,* Invent. Math. 33 (1976), 223–246.

[2] E. Cartan, *Sur le groupe de la géométrie hypersphérique,* Comment. Math. Helv. 4 (1932), 158–171.

[3] M. Deraux and E. Falbel, *The complex hyperbolic geometry of the figure eight knot,* preprint, 2013.

[4] E. Falbel, *A spherical CR structure on the complement of the figure eight knot with discrete holonomy,* J. Differential Geom. 79 (2008), 69–110.
[5] E. Falbel and N. Gusevskii, *Spherical CR-manifolds of dimension 3,* Bol. Soc. Brasil. Mat. (N. S.) 25 (1994), no. 1, 31–56.
[6] E. Falbel and J. Parker, *The geometry of the Eisenstein–Picard modular group,* Duke Math. J. 131 (2006), no. 2, 249–289.
[7] W. M. Goldman, *Complex hyperbolic geometry,* Oxford Mathematical Monographs, Oxford Science Publications, The Clarendon Press, Oxford University Press, New York, 1999.
[8] H. Jacobowitz, *An introduction to CR structures,* Math. Surveys Monogr., 32, American Mathematical Society, Providence, RI, 1990.
[9] J.-P. Otal, *Le théorème d'hyperbolisation pour les variétés fibrées de dimension 3,* Astérisque 235 (1996).
[10] J. Parker and P. Will, in preparation.
[11] A. Reid, private communication.
[12] R. E. Schwartz, *Spherical CR geometry and Dehn surgery,* Ann. of Math. Stud., 165, Princeton University Press, Princeton, NJ, 2007.
[13] T. Zhao, *Generators for the Euclidean Picard modular groups,* Trans. Amer. Math. Soc. 364 (2012), 3241–3263.

Institut de Mathématiques de Jussieu
Unité Mixte de Recherche 7586 du CNRS
Université Pierre et Marie Curie
4, place Jussieu
75252 Paris Cedex 05
France

elisha.falbel@imj-prg.fr

College of Mathematics and Econometrics
Hunan University
Changsha, 410082
People's Republic of China

jywang@hnu.edu.cn